JGR Biogeosciences

RESEARCH ARTICLE
10.1029/2022JG007027

Key Points:

- Species-specific tree dissolved organic matter evaded microbial consumption and survived watershed transit to enter the marine environment
- Ultrahigh-resolution mass spectrometry showed homogenized organic material in spring and aromatic, freshly leached material in summer
- Antecedent watershed conditions like plant growth stage may influence organic matter source availability and flow connectivity

Supporting Information:

Supporting Information may be found in the online version of this article.

Correspondence to:

M. I. Behnke,
mibehnke@alaska.edu

Citation:

Behnke, M. I., Fellman, J. B., D'Amore, D. V., & Spencer, R. G. M. (2023). Trees in the stream: Determining patterns of terrestrial dissolved organic matter contributions to the northeast Pacific coastal temperate rainforest. *Journal of Geophysical Research: Biogeosciences*, *128*, e2022JG007027. https://doi.org/10.1029/2022JG007027

Received 2 JUN 2022
Accepted 4 APR 2023

Trees in the Stream: Determining Patterns of Terrestrial Dissolved Organic Matter Contributions to the Northeast Pacific Coastal Temperate Rainforest

M. I. Behnke[1,2], J. B. Fellman[2], D. V. D'Amore[3], and R. G. M. Spencer[1]

[1]National High Magnetic Field Laboratory Geochemistry Group and Department of Earth, Ocean, and Atmospheric Science, Florida State University, Tallahassee, FL, USA, [2]Department of Natural Sciences and Alaska Coastal Rainforest Center, University of Alaska Southeast, Juneau, AK, USA, [3]USDA Forest Service, Pacific Northwest Research Station, Juneau, AK, USA

Abstract Dissolved organic matter (DOM) composition in small watersheds depends on complex antecedent conditions that ultimately influence DOM generation, processing, and stability downstream. Here, we used ultrahigh resolution Fourier-transform ion cyclotron resonance mass spectrometry and total dissolved nitrogen and dissolved organic carbon concentrations to investigate how DOM is produced in distinct sub-catchment types (poor fen, forested wetland, and upland forest) and transported through a watershed in the northeast Pacific coastal temperate rainforest (NPCTR). We traced a suite of previously identified source-specific marker formulae from vegetation and soil downstream and used them to test models of terrestrial DOM inputs. Marker formulae escaped microbial degradation and were exported from the watershed, demonstrating strong land-to-ocean connectivity through the transfer of unmodified tree DOM from specific tree species into the marine environment. Simple hydrologic and temperature variables were better able to predict inputs of soil-sourced DOM into the stream network than tree-sourced DOM, highlighting the role of antecedent conditions (e.g., plant growth stage) in DOM source availability and hydrologic flow connectivity, particularly for plant-derived material. Forested wetland pore waters featured thousands of nitrogen-containing molecular formulae that potentially provide a path of direct organic nitrogen uptake to organisms. The modified aromaticity index peaked in midsummer (up to 0.55 for fen headwaters) suggesting DOM inputs from freshly produced vegetation provide a strong summertime terrestrial signal. As the climate changes, new watershed-scale conditions may further complicate predictions of DOM source availability, flow connectivity, and downstream fate in NPCTR watersheds.

Plain Language Summary The signature of dissolved organic matter molecules affects what role they play in the ecosystem, such that molecular shape influences ecosystem productivity and the global carbon cycle. Molecular signature can depend on both the source of the dissolved organic matter and on what happens to it. Some studies in controlled laboratory environments have suggested that the ways dissolved organic matter changes shape as microbes interact with it removes the unique properties its source provided it with. In this study, we measured dissolved organic matter throughout a watershed in Southeast Alaska to see how it changes as it moves from sources on land through stream systems. We found that certain specific dissolved organic matter types that come from specific plant species and soil layers make it to the stream mouth without being changed along the way. This shows that original source can be more important than processing history for molecular signature. The relationship between the amount of stream discharge and the source-specific dissolved organic matter was complicated and suggests that the conditions leading up to the specific sampling time (like soil moisture levels or plant growth stage) have a strong impact on the type and fate of dissolved organic matter.

1. Introduction

The origins and degradation history of dissolved organic matter (DOM) control its chemical composition and thus its role in the carbon cycle (Hansen et al., 2016; Opsahl & Benner, 1997; Shirokova et al., 2019; Wagner et al., 2019). Substantial research has focused on environmental transformations of DOM (e.g., Fasching et al., 2014; Stubbins & Dittmar, 2015) and on the links between landscape sources and DOM composition (e.g., Laudon et al., 2011; Sanderman et al., 2009; Van Stan et al., 2017). Laboratory studies of DOM from various terrestrial sources have suggested that the processing that occurs after DOM has entered stream networks can be

as important as the original composition dictated by the DOM source for controlling the potential composition and fate of DOM after export to downstream environments (e.g., D'Andrilli et al., 2019; Hansen et al., 2016). Such research has led to the hypothesis that microbes may homogenize terrestrial-derived DOM along the flow network and thus buffer changes in DOM composition due to modified source inputs from watershed perturbations like landcover change (Harfmann et al., 2019; Rossel et al., 2013). However, just as bottle effects (e.g., Ferguson et al., 1984; Nevalainen et al., 2020) may modify microbial response and DOM chemistry in artificially confined experiments, such in vitro studies cannot account for the complexity of conditions that DOM encounters as it transits the terrestrial-aquatic interface. Variables like discharge, source availability, soil flow path, and redox potential (e.g., D'Amore et al., 2015; Wagner et al., 2019; Wollheim et al., 2018) may impact whether microbial homogenization of DOM occurs along flow networks. These field-based measurements can thus support or help correct specious conclusions from laboratory experiments about the character and behavior of source-specific DOM throughout a watershed.

The northeast Pacific coastal temperate rainforest (NPCTR) is an excellent setting for evaluating the role of stream processing on DOM composition. The ecosystem is a hotspot for carbon storage with areas of aboveground biomass approaching 950 Mg ha^{-1} and regional soil organic carbon stocks averaging 228 ± 111 Mg ha^{-1} (Buma et al., 2016; Heath et al., 2011; McNicol et al., 2019). These high carbon densities combined with the abundant precipitation in the region fuel substantial stream export of DOM. The Southeast Alaskan portion of the NPCTR alone yields a flux of DOM (~1.2 Tg C yr^{-1} measured as dissolved organic carbon; DOC; Edwards et al., 2021) equivalent to ~20% of the ~8.1 Tg C yr^{-1} DOC flux of the entire contiguous United States (Stets & Striegl, 2012), a region ~5,100% larger than the NPCTR. The fates of this large DOM flux in the marine environment may vary depending on its composition, making the study of DOM source and compositional control in the NPCTR valuable both on a watershed and regional carbon-cycling level.

Fourier-transform ion cyclotron resonance mass spectrometry (FT-ICR MS) provides both broad characterization of DOM by compound classes and bulk metrics (e.g., Johnston et al., 2020; Sleighter & Hatcher, 2008) and detailed observation of specific molecular formulae (e.g., Lechtenfeld et al., 2014; Wagner et al., 2019). Thus, FT-ICR MS allows molecular-level analysis of DOM across hydrologic changes (e.g., Wagner et al., 2019) and across specific sources (e.g., Stubbins et al., 2017). Molecular formulae identified by FT-ICR MS have previously been conceptualized as tracers of specific DOM inputs to surface waters or of specific processing pathways (Bercovici et al., 2018; Bhatia et al., 2010; Hertkorn et al., 2016; Lechtenfeld et al., 2014). FT-ICR MS thus allows molecular level insight into DOM inputs and is a useful technique for identifying specific tracer formulae derived from different DOM sources or processes in situ. FT-ICR MS data have also been shown to correlate to other organic matter properties (e.g., isotopic composition, element ratios, etc; Behnke et al., 2020; Flerus et al., 2012; Poulin et al., 2017; Seidel et al., 2015), enabling comparison between molecular properties and surrounding environmental variables, like changing land cover and precipitation patterns. FT-ICR MS further allows molecular-level analysis of DOM across hydrologic changes, which can control the coupling of groundwater or soil pore water DOM with streamwater DOM (Raymond & Saiers, 2010; Wagner et al., 2019; Walvoord & Striegl, 2007; Wollheim et al., 2018).

In this study, our goal was to investigate whether terrestrially sourced DOM can persist throughout a watershed without ceding its initial composition to in-stream processing. Further, we examined how terrestrial DOM inputs can vary with season and location in a watershed at both the bulk composition level and with respect to individual molecular formulae. To do this, we used FT-ICR MS combined with the concentrations of DOC and total dissolved nitrogen (TDN) to explore the transfer and tracing of DOM from multiple terrestrial sources into the stream network in Aangooxa Yé (referred to in past studies as Fish Creek) watershed near Juneau, Alaska (Figure 1). We measured DOM composition throughout the watershed, sampling the mainstem river above tidal influence and soil pore waters and tributary streams from sub-catchments draining three main landscape units in the NPCTR (poor fen, forested wetland and upland forest; D'Amore et al., 2015; McNicol et al., 2019). We applied previously identified source-specific marker formulae from the Aangooxa Yé watershed (Behnke et al., 2022) to our fluvial data set to trace DOM from specific sources in the stream network. We used the presence/absence of source-specific marker formulae along the fluvial network as an indicator of DOM uptake or transformation based on the behavior of source-specific DOM in our previous bioincubations. Finally, we evaluate whether source-specific formulae occurrences and the modified aromaticity index (AI_{mod}; a metric of unsaturation based on molecular formulae) of each DOM sample can be modeled using basic hydrologic and temperature variables across the main discharge season.

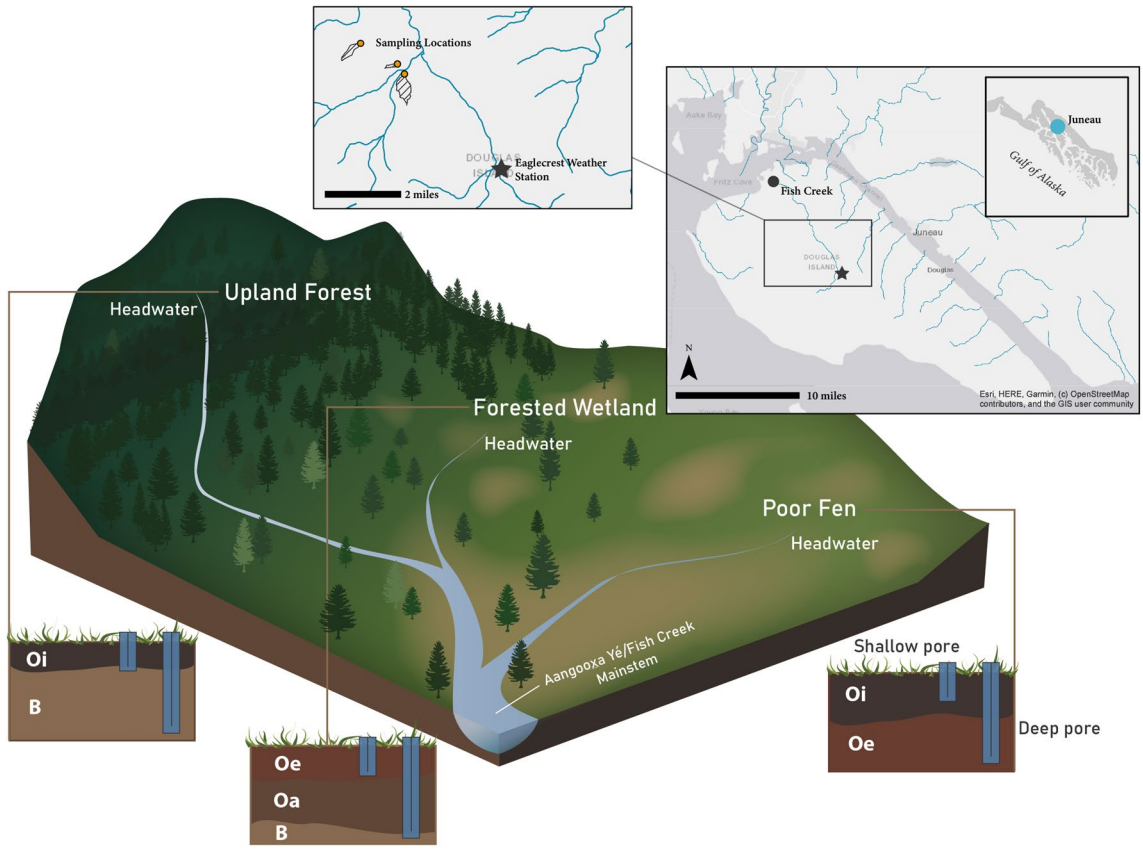

Figure 1. Location and sampling design for the three landscape types in Aangooxa Yé/Fish Creek watershed near Juneau, Alaska. Headwaters were sampled for each sub-catchment, and the mainstem was sampled near the mouth. Sampled shallow and deep soil pore waters for upland forest, forested wetland, and poor fen are shown in representative soil layers. The adjacent weather station at Eaglecrest is shown at the star.

2. Methods

2.1. Site Description

Sampling took place in three sub-catchments occupied by dominant landscape types in Aangooxa Yé watershed near Juneau, Alaska from May through October of 2018 (Figure 1). The climate is moderate and maritime with cool summers, mild winters, and substantial precipitation (~2,000 mm) at sea level. Aangooxa Yé (36 km^2; 487 m mean elevation) features temperate rainforest, wetlands, and alpine zones and rests on intrusive volcanic and sedimentary rock in the Stephens Passage volcanic subsection (D'Amore et al., 2015).

The sub-catchments span a common soil drainage gradient in the NPCTR. The poor fen has a mean elevation of 253 m, a mean slope of 6.6%, and an estimated soil C stock of 556 Mg C ha^{-1}. The poor fen is a mostly unforested poorly drained slope bog wetland type with peat accumulation of >2m and acidic (pH < 4.0) soils (D'Amore et al., 2015; Fellman et al., 2008; National Wetlands Working Group, 1988). The forested wetland is a raised peatland swamp with an overstory of western hemlock (*Tsuga heterophylla*) and Sitka spruce (*Picea sitchensis*) (National Wetlands Working Group, 1988), and contains acidic (pH < 4.0) soils with 0.50–0.75 m deep peat overlying glacial till (D'Amore et al., 2015; Fellman et al., 2008). The site has a mean elevation of 240 m, a mean slope of 15.5%, and an estimated soil carbon content of 376 Mg C ha^{-1}. The forested wetland has greater soil hydraulic conductivity than does the poor fen (which is underlain by the same deposit) yet maintains adequate saturation for anoxic conditions to be regularly present (D'Amore et al., 2010). The upland forest also has a western hemlock and Sitka spruce overstory. The site has a mean elevation and slope of 392 m and 19.4%, respectively and an estimated soil carbon content of 245 Mg C ha^{-1}. The upland features deep and well drained acidic (pH < 4.0) Spodosols on steep slopes (D'Amore et al., 2015; Fellman et al., 2008).

2.2. Temperature, Precipitation, Discharge, Water Table, and Seasonality

Temperature and precipitation data for 2018 were obtained from the National Weather Service Cooperative Observer Program weather station at Eaglecrest Base, Juneau, AK, in Aangooxa Yé watershed at a similar elevation and adjacent to the sampling sites (Figure 1). Mean ± standard error of daily air temperatures was calculated for each month, and the lowest temperature recorded was used to assess months when temperatures in the watershed dropped below freezing. Daily measurements of rainwater equivalent precipitation (cm) were also summed to examine monthly totals.

Discharge in the mainstem of Aangooxa Yé ("mainstem") was recorded every 15 min with a pressure transducer (In Situ Level TROLL) in a stilling well. A SonTek FlowTracker ADV was used to determine discharge measurements across a wide range of flow conditions during the sampling period (May–October) of 2018. The stage-discharge relationship was used to calculate streamflow during the sampling period when stage-discharge relationships were actively assessed (Fellman et al., 2020). Water table in each sub-catchment was tracked using stilling wells in each outlet stream (near the "head" sampling locations). Hobo model U20 pressure transducers were used to record water height every 30 min and corrected for atmospheric pressure. Stage-discharge relationships were not quantified in the sub-catchment streams due to an insufficient number of flow measurements at each site. However, changes in water pressure corrected for atmospheric pressure are here used as a proxy to assess relative fluctuations in stage height in each sub-catchment.

For Aangooxa Yé watershed, we consider the months when mean daily air temperature (Table S1 and Figure S1 in the Supporting Information S1) falls below freezing as winter (December-April), the months in which mean daily temperature is above freezing but low temperatures dip below freezing as spring (May), above freezing months as summer (June-August), and months where again there are dips below freezing but mean daily temperature stays above freezing (and snow begins to occur) as fall. These delineations match the previously identified hydrologic periods present during the main runoff season (e.g., not during winter): spring snowmelt (May), summer draw-down period (June-early August, when our August sampling occurred), and fall wet season (late August-November) (Fellman, Hood, D'Amore, et al., 2009).

2.3. Soil Pore Water and Stream Sampling

Monthly sampling occurred for 6 months at 10 sites around the watershed (the headwater site and shallow and deep pore water waters for each sub-catchment, plus the mainstem; Figure 1). Acid-washed Tygon tubing and inline pre-combusted (>4 hr at 450 ºC) Whatman GF/F filters (0.7 µm pore size) in a battery-operated pump were used to collect tributary stream water and mainstem water near the mouth of Aangooxa Yé. Soil water was sampled from triplicate 25 and 50 cm depth wells and combined to create one shallow pore water and one deep pore water sample from each site on each sampling date. Sampling wells thus collected water moving through the soil horizons at 25 or 50 cm (see Figure 1 for a map of approximate soil horizon locations for each site). Wells were made of 3.2 cm diameter polyvinyl chloride tubing, slotted at 25 and 50 cm (D'Amore et al., 2015). A hand auger of smaller diameter was used to remove soil and wells were placed in each hole, followed by a 1-month equilibration period before sampling began. The inline filter and Tygon tubing pump were also used to acquire samples from wells. Since the water table in the fen and forested wetland sites was often within 10–20 cm of the soil surface, wells primarily sampled water from the saturated zone. However, for the purpose of this study, we refer to all water collected from the wells as soil pore water.

2.4. Concentrations of DOC and TDN

Filtered water samples for DOC and TDN were acidified (pH 2) and stored refrigerated in pre-combusted (>4 hr at 550 ºC) amber glass vials until analysis within 48 hr of collection. DOC and TDN concentrations of acidified and sparged samples were determined on a Shimadzu TOC-L CSH/CSN analyzer using high-temperature combustion (Fellman, Hood, D'Amore, et al., 2009).

2.5. Fourier-Transform Ion Cyclotron Mass Spectrometry

Reverse phase BondElut Priority PolLutant (PPL) columns (100 mg; Agilent) were used for sample solid-phase extraction (Dittmar et al., 2008). Acidified (pH 2) samples with carbon normalized volumes (40 µg C mL^{-1} target

concentrations) were passed through pre-cleaned PPL columns, eluted in JT Baker HPLC grade methanol, and stored at −20° C. Analysis occurred on a custom-built FT-ICR MS equipped with a passively shielded 9.4 T magnet (Oxford Instruments, Abington, Oxfordshire, U.K.) at the National High Magnetic Field Laboratory (Tallahassee, Florida, USA; Kaiser et al., 2011; Stenson et al., 2003) with direct infusion negative electrospray ionization. Each mass spectrum collected consisted of 100 coadded time domain acquisitions.

Molecular formulae were assigned for peaks with >6σ root-mean-square baseline noise with previously described guidelines (Koch et al., 2007) with PetroOrg ©™ software (Corilo, 2015). Formulae assignment boundaries were $C_{1\text{-}45}H_{1\text{-}92}N_{0\text{-}4}O_{1\text{-}25}S_{0\text{-}2}$ and a mass accuracy ≤300 ppb (Kellerman et al., 2018). The modified aromaticity index (AI_{mod}; used to assess the degree of unsaturation based on molecular formula) was calculated (Koch & Dittmar 2006, 2016) and used (with elemental ratios) to assign compound classes: polyphenolics ($0.5 < AI_{mod} \leq 0.66$); condensed aromatics ($AI_{mod} > 0.66$); highly unsaturated and phenolic ($AI_{mod} \leq 0.5$, $H/C < 1.5$, $O/C \leq 0.9$; HUPs); aliphatics ($1.5 \leq H/C \leq 2.0$, $O/C \leq 0.9$ and $N = 0$); N-containing aliphatic compounds (also known as peptide-like formulae; $1.5 \leq H/C \leq 2.0$, $O/C \leq 0.9$ and $N > 0$); and sugar-like ($O/C > 0.9$). Here, "compound" refers to the different isomers each unique formula may represent (Hertkorn et al., 2007) rather than a specific isomer and is used in reference to compound classes only. Relative abundances of formulae were found by normalizing individual peak magnitudes to the sum of all assigned peaks for each sample. The contributions of the compound classes are expressed as percentages and were calculated as the sum of all the relative abundances for each peak in each compound class divided by the summed abundances of all assigned formulae in each sample. Similar calculations determined the relative abundances of compounds containing different elements (e.g., CHO, CHON, CHOS, CHONS). The PPL method isolates a subset of the bulk DOM pool and FT-ICR MS via negative electrospray preferentially ionizes aromatic carboxylic acids, thereby representing only a subset of the total DOM (Kurek et al., 2023). Previous studies however have shown this fraction of DOM to scale quantitatively with aromaticity, carbon age, and heteroatom content (e.g., Behnke et al., 2020; Kellerman et al., 2018; Poulin et al., 2017), and thus using this technique makes this work directly comparable to other molecular-level studies of DOM (e.g., Hertkorn et al., 2016; Wagner et al., 2019; Yang et al., 2022).

A recent study in the Aangoo̲xa Yé watershed defined a list of source-specific marker formulae (ranging from 1 to 176 formulae for each of 10 sources identified; Table S2 in the Supporting Information S1) that were here used to pinpoint source marker formulae in this sample set (Behnke et al., 2022). The number of marker formulae in each sample was assessed. Further, seasonally unique formulae were identified in this data set as formulae present in only one sampling month but in more than two samples from that time period.

2.6. Statistical Analyses

Descriptive statistics were used to assess patterns in DOC and TDN concentration and DOM composition between sites and across the sampling period. Generalized linear models were used to assess whether continuous hydrologic or temperature variables (24 hr precipitation in cm, 48 hr precipitation in cm, mainstem discharge in cubic meters per second or cms, mean daily temperature in °C), location (headwater, shallow pore water, deep pore water), or site (poor fen, forested wetland, upland, or mainstem) significantly impacted several FT-ICR MS measurements of terrestrial connectivity: (a) the bulk metric AI_{mod} weighted average, (b) the number of source-specific marker formulae identified in each sample, (c) the number of spruce stemflow-specific marker formulae identified in each sample, and (d) the number of marker formulae from any soil layer identified in each sample. Aromatic formulae such as condensed aromatics and polyphenolics have been shown to be sourced predominantly from terrestrial plant material (DiDonato et al., 2016; Johnston et al., 2020; Kellerman et al., 2018) including in Southeast Alaska (Behnke et al., 2020; Holt et al., 2021), so AI_{mod} (measuring aromaticity; Koch & Dittmar, 2006, 2016) was chosen as a bulk measure of terrestrial connectivity. Source-specific marker formulae that have been shown to come from a single organic matter source in the NPCTR (Behnke et al., 2022) were chosen as a more detailed assessment of terrestrial connectivity, both assessed in bulk and by main source type. For AI_{mod}, Gaussian linear models were fit in base *R* using the glm() function (R Core Team, 2019). For source-specific formulae, negative binomial models were run using the *MASS* package (Venables & Ripley, 2002) to account for count data where the mean is not assumed equal to the variance. Possible models were compared using the change in finite sample corrected Akaike's Information Criterion (ΔAIC_c) using the *AICcmodavg* package (Mazerolle, 2019). This approach determines which model has the highest likelihood given the data while penalizing unnecessary parameters, thus best balancing bias and variance (Burnham & Anderson, 2002).

Table 1
Mean ± Standard Error for Stream and Soil Pore Water for DOC and TDN Concentrations, DOC:TDN Ratio, and FT-ICR MS Metrics and Compound Classes (Expressed as Percent Relative Abundances)

Site	Fish	Fen			Forested wetland			Upland	
Position	Mainstem	Headwaters	Shallow pore water	Deep pore water	Headwaters	Shallow pore water	Deep pore water	Headwaters	Deep pore water
n (FT-ICR)	6	6	6	6	6	6	6	6	4
DOC $mgCL^{-1}$	4.3 ± 1.1	17.4 ± 1.7	16.3 ± 1.3	15.0 ± 1.0	12.1 ± 1.2	30.1 ± 4.4	33.3 ± 3.0	1.8 ± 0.3	18.1 ± 3.1
TDN $mgNL^{-1}$	0.1 ± 0.0	0.2 ± 0.0	1.2 ± 0.9	1.10 ± 0.9	0.1 ± 0.0	1.4 ± 0.7	2.2 ± 0.8	0.0 ± 0.0	0.2 ± 0.0
DOC:TDN	31.6 ± 6.6	83.8 ± 4.0	51.4 ± 12.9	52.8 ± 10.9	84.6 ± 1.3	40.8 ± 10.0	29.0 ± 10.3	49.9 ± 4.7	81.9 ± 16.7
AI_{mod}	0.39 ± 0.01	0.43 ± 0.03	0.42 ± 0.02	0.41 ± 0.02	0.42 ± 0.01	0.41 ± 0.01	0.40 ± 0.02	0.36 ± 0.01	0.39 ± 0.02
CHO	90.0 ± 1.1	92.8 ± 1.0	94.1 ± 0.6	93.9 ± 1.1	92.8 ± 0.7	92.6 ± 0.3	91.8 ± 0.5	91.9 ± 1.1	92.5 ± 1.7
CHON	5.0 ± 0.2	3.9 ± 0.4	3.3 ± 0.2	3.7 ± 0.6	3.8 ± 0.3	4.0 ± 0.3	5.5 ± 0.5	4.5 ± 0.6	3.0 ± 0.9
CHOS	4.3 ± 1.1	2.3 ± 0.6	1.8 ± 0.4	1.7 ± 0.4	2.3 ± 0.5	2.6 ± 0.6	2.3 ± 0.3	3.2 ± 0.5	3.7 ± 1.1
CHONS	0.6 ± 0.3	1.0 ± 0.2	0.8 ± 0.2	0.7 ± 0.2	1.1 ± 0.2	0.9 ± 0.2	0.4 ± 0.1	0.5 ± 0.2	0.8 ± 0.2
Condensed aromatics	7.9 ± 1.6	12.2 ± 3.8	12.0 ± 3.4	9.2 ± 1.8	11.3 ± 1.7	10.4 ± 1.6	8.1 ± 2.2	4.9 ± 1.0	9.5 ± 2.3
Polyphenolics	15.3 ± 1.5	20.6 ± 2.2	19.5 ± 2.5	20.1 ± 2.3	19.0 ± 1.1	18.7 ± 1.3	18.4 ± 1.7	10.7 ± 1.4	16.2 ± 2.4
Aliphatics	3.1 ± 0.8	1.9 ± 0.4	2.2 ± 0.3	2.6 ± 0.4	1.9 ± 0.2	2.5 ± 0.3	2.5 ± 0.2	1.8 ± 0.2	4.1 ± 1.9
Peptide-like	0.2 ± 0.1	0.2 ± 0.1	0.1 ± 0.0	0.2 ± 0.1	0.1 ± 0.1	0.2 ± 0.1	0.3 ± 0.1	0.2 ± 0.1	0.2 ± 0.1
Sugar-like	0.4 ± 0.0	0.6 ± 0.2	0.4 ± 0.1	0.4 ± 0.1	0.5 ± 0.1	0.6 ± 0.1	0.6 ± 0.1	0.2 ± 0.0	0.8 ± 0.2
HUPs	73.1 ± 3.4	64.5 ± 5.7	65.8 ± 5.6	67.6 ± 3.7	67.2 ± 2.8	67.6 ± 2.7	70.1 ± 3.7	82.2 ± 2.5	69.3 ± 3.2

3. Results

3.1. Climate and Watershed Hydrology

Precipitation occurred throughout the year in rain events typical of the region (Figure S1 in the Supporting Information S1; Fellman et al., 2020; Pierre et al., 2020). October was the wettest month and March the driest (35.1 v. 11.0 cm water equivalent, respectively). During the measured period, discharge in the mainstem tracked precipitation with peak flows followed by slowly decreasing baseflows until the next precipitation event (Figure S1 in the Supporting Information S1). The exception occurred in May, when snowmelt from higher watershed elevations inflated mainstem discharge and stage height levels in the sub-catchments streams independent of precipitation amounts (D'Amore et al., 2010). This snowmelt contribution to discharge further separated the spring season from the summer season. Of the measured period, the greatest mean discharge occurred in spring (May: 3.6 m^3s^{-1}) and fall (October: 3.2 m^3s^{-1}) as is generally typical of non-glacial catchments in the region (Edwards et al., 2021). In all three sub-catchments, pressure transducers showed roughly similar patterns in stage height, influenced by the distinct soil properties of each watershed (Figure S2 in the Supporting Information S1). Stage height in all three sub-catchments was similar to the mainstem in the timing of their precipitation-driven increases and decreases as previously observed (D'Amore et al., 2015), though the fen and upland have muted responses to precipitation.

3.2. DOC and TDN Concentrations and DOC:TDN

Concentrations of DOC were highest in the forested wetland pore waters (33.3 ± 3.0 and 30.1 ± 4.4 $mgCL^{-1}$, mean ± standard error, for deep and shallow pore water; Table 1; Figure 2a). Mean DOC was lowest in the mainstem and upland stream (4.3 ± 1.1 and 1.8 ± 0.3 $mgCL^{-1}$, respectively), fitting with previously observed variations between sub-catchment soil and streamwater in the region (Fellman et al., 2008). Broadly, stream and pore water DOC were lowest in the spring and fall and peaked in summer (Figures 3a–3d).

Soil and streamwater TDN concentrations showed a similar pattern to that of DOC across sites. Concentrations of TDN were comparable between the forested wetland deep and shallow pore waters (2.2 ± 0.8 and 1.4 ± 0.7 $mgNL^{-1}$). All other sites had low (<0.2 $mgNL^{-1}$) or negligible concentrations (Table 1; Figure 2b;

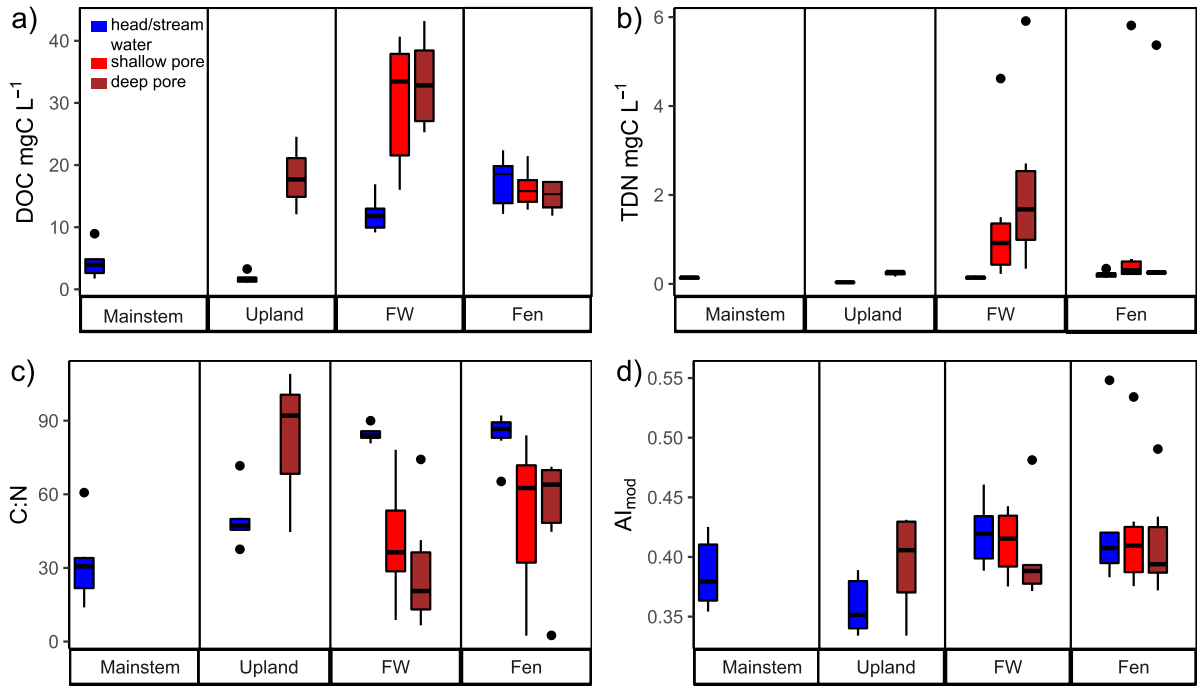

Figure 2. Soil pore water and streams (a) dissolved organic carbon (DOC) concentrations, (b) TN concentrations, (c) C:N ratios, and (d) AI_{mod} weighted averages for sites across the sampling period. FW stands for forested wetland. The horizontal line represents the median, the 25th and 75th percentiles are either side of the boxes, and whiskers go to the minimum or maximum value or 1.5 times the interquartile range past the box (whichever is nearer the median). Outlying points past the whiskers' range are black dots.

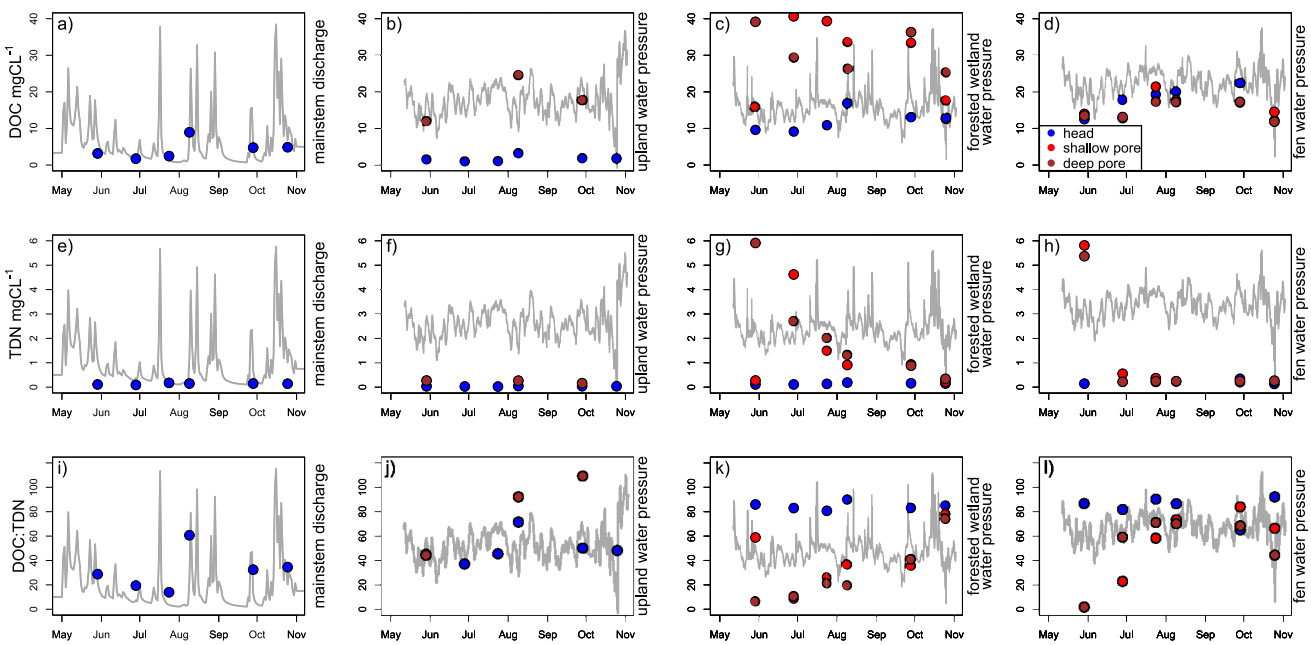

Figure 3. Dissolved organic carbon (DOC) (a–d), total dissolved nitrogen (TDN) (e–h), and C:N ratios for DOM (i–l) for sampling period. Mainstem (a,e,i), upland (b,f,j), forested wetland (c,g,k) and fen (d,h,l) data for stream samples (blue dots), shallow pore samples (red dots), and deep pore samples (brown dots). For mainstem panels, Aangooxa Yé mainstem discharge is shown, while for sub-catchment panels sub-catchment water table pressure is shown. Water pressure and discharge are for reference and are not to scale.

Fellman et al., 2008). Stream and pore water TDN was low (<0.4 $mgNL^{-1}$) throughout the sampling season, except for the forested wetland deep pore water and fen shallow and deep pore waters where TDN peaked in May (5.9, 5.8, 5.4 $mgNL^{-1}$, respectively), and in the forested wetland shallow pore water (with a June peak of 4.6 $mgNL^{-1}$; Figures 3e–3h). Concentrations of TDN then substantially decreased in the fen pore waters and decreased more slowly across the entire sampling period in the forested wetland pore waters.

The forested wetland headwater had the highest mean DOC:TDN and the forested wetland deep pore water had the lowest (84.6 ± 1.3 vs. 29.0 ± 10.3; Table 1; Figure 2c). The seasonal pattern in DOC:TDN varied between stream and pore water samples (Figures 3i–3l). Pore water samples had lowest DOC:TDN in May except for the forested wetland shallow pore water where the minimum fell in June, and generally increased throughout the summer with a small decrease again in fall in the fen.

3.3. FT-ICR MS Data, Heteroatomic Content, and Compound Classes

FT-ICR MS metrics and compound class averages and seasonal patterns were similar between sites (Table 1; Figure 4). Mean AI_{mod} had a narrow range, from 0.36 ± 0.01 in the upland headwater to 0.43 ± 0.03 in the fen headwater (Figure 2d). AI_{mod} peaked in late July/early August (up to 0.55 in fen headwater), except for the upland deep pore water where it was equivalent in May and early August (Figures 5a–5d).

The largest number of formulae were found in the upland headwaters (mean ± standard deviation: 9,527 ± 2,400), while fen shallow pore water had the least (7,212 ± 826). Mainstem samples showed an intermediate value (8,812 ± 1,310). In general, fewer formulae were found in pore water samples and more in headwaters, but there were exceptions to both trends (Table S3 in the Supporting Information S1). There were 885 formulae present in all samples at all times, of which 595 were HUPs, 91 were condensed aromatics, 162 were polyphenolics, 29 were aliphatics, and 8 were sugar-like. Fen shallow pore water had the greatest mean CHO presence (94.1 ± 0.6%RA), while the fen deep pore water reached the data set maximum of 98.9%RA in August (Table 1; Figure 4; Figure S2 in the Supporting Information S1). The mainstem had the lowest mean CHO contribution (90.0 ± 1.1%RA) and reached the lowest value in the sample set (86.4%RA) in May. Mean CHON contribution ranged from 3.0 ± 0.9%RA in the upland deep pore water to 5.5 ± 0.5%RA in the forested wetland deep pore water, reaching a maximum value there of 7.6%RA in June. Mean CHOS contribution was lowest in the fen deep pore water and highest in the mainstem (1.7 ± 0.4 and 4.3 ± 1.1%RA). CHONS containing formulae comprised <2%RA in all samples.

Mean contribution of condensed aromatics and polyphenolics were greatest in the fen headwater (12.2 ± 3.8 and 20.6 ± 2.2%RA, respectively) and lowest in the upland headwater (4.9 ± 1.0 and 10.7 ± 1.4, respectively; Table 1; Figure 4). Sites followed similar patterns, with a peak contribution of these classes in mid-summer (Figure S2 in the Supporting Information S1). Upland deep pore water had the highest mean aliphatic %RA and the upland headwater had the lowest (4.1 ± 1.9 and 1.8 ± 0.2). Sugar-like and peptide-like formulae always made up <2 and <1%RA, respectively. Highly unsaturated and phenolic formulae make up the bulk %RA of all sites, with means ranging from 82.2 ± 2.5 in the upland headwater to 64.5 ± 5.7 in the fen headwater.

3.4. Source-Specific and Seasonally Unique Molecular Formulae

As noted above, a recent study described 252 source-specific marker formulae leached from specific soil horizons and plant types in the study watershed (Table S2 in the Supporting Information S1; Behnke et al., 2022). These marker formulae, the majority of which (176) originated from spruce stemflow, occurred in all samples of a given source and in no samples of any other sources (Behnke et al., 2022). All 252 source-specific marker formulae were found in this watershed data set. Spruce stemflow source-specific formulae (which comprised ~70% source-specific formulae previously identified) made up >90% of the occurrences of a source-specific formulae here. Formulae leached from the upland O_i organic soil horizon made up ~7% source-specific formulae occurrences, with the forested wetland O_a soil horizon providing another ~1%. The other sources (epiphytes, hemlock throughfall, spruce bark, and fen O_e and O_i and upland B soil horizons) each contributed <1%. The stream samples had a greater occurrence of source-specific formulae over the course of the summer than did their respective sub-catchment pore waters, with the upland headwater and mainstem proving most abundant (266 and 234 instances, respectively; Figures 5e–5h). Across all sites for each sampling time, late July had the greatest occurrence of source-specific marker formulae (424 instances; Figure 5). Though each sampling location had a unique pattern of source-specific marker formulae timing, peak occurrences mostly appear in either July or fall (Figures 5e–5h). Across all sites, the June and August samplings contained the least instances of source-specific formulae.

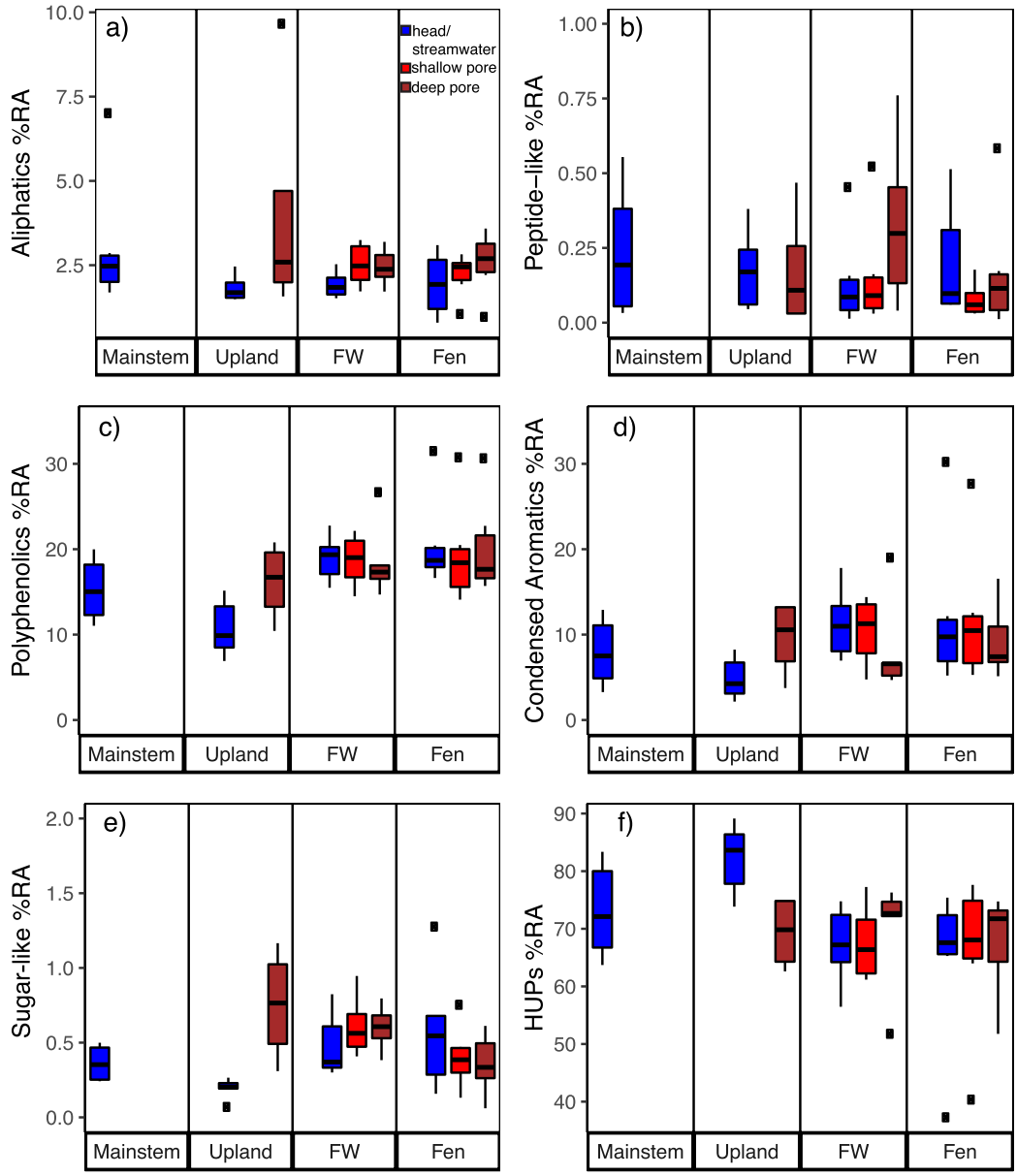

Figure 4. Fourier-transform ion cyclotron resonance mass spectrometry (FT-ICR MS) compound classes throughout the sampling season. The horizontal line represents the median, the 25th and 75th percentiles are either side of the boxes, and whiskers go to the minimum or maximum value or 1.5 times the interquartile range past the box (whichever is nearer the median). Outlying points past the whiskers' range are black dots.

The number and extent of unique seasonal molecular formulae were low in spring, peaked in early August, and declined into fall (Table 2; Figure S3 in the Supporting Information S1). There were 697 formulae that appeared only in August and in more than one site, including 37 formulae appearing in four sites and six formulae in 5 sites, or more than half of sampling locations. Condensed aromatics and polyphenolics comprise a greater percent of the number of the unique formulae in August than in any other month (~54% and ~29%, respectively).

3.5. Modeling Terrestrial Connectivity Using Hydrologic Variables and FT-ICR MS Data

There was model uncertainty ($\Delta AIC_c < 2$) between six of the 12 assessed models tested to determine the impact of continuous hydrologic and temperature variables on the total number of source-specific formulae present in a sample (Table S4 in the Supporting Information S1). Those six models featured daily precipitation, 48-hr

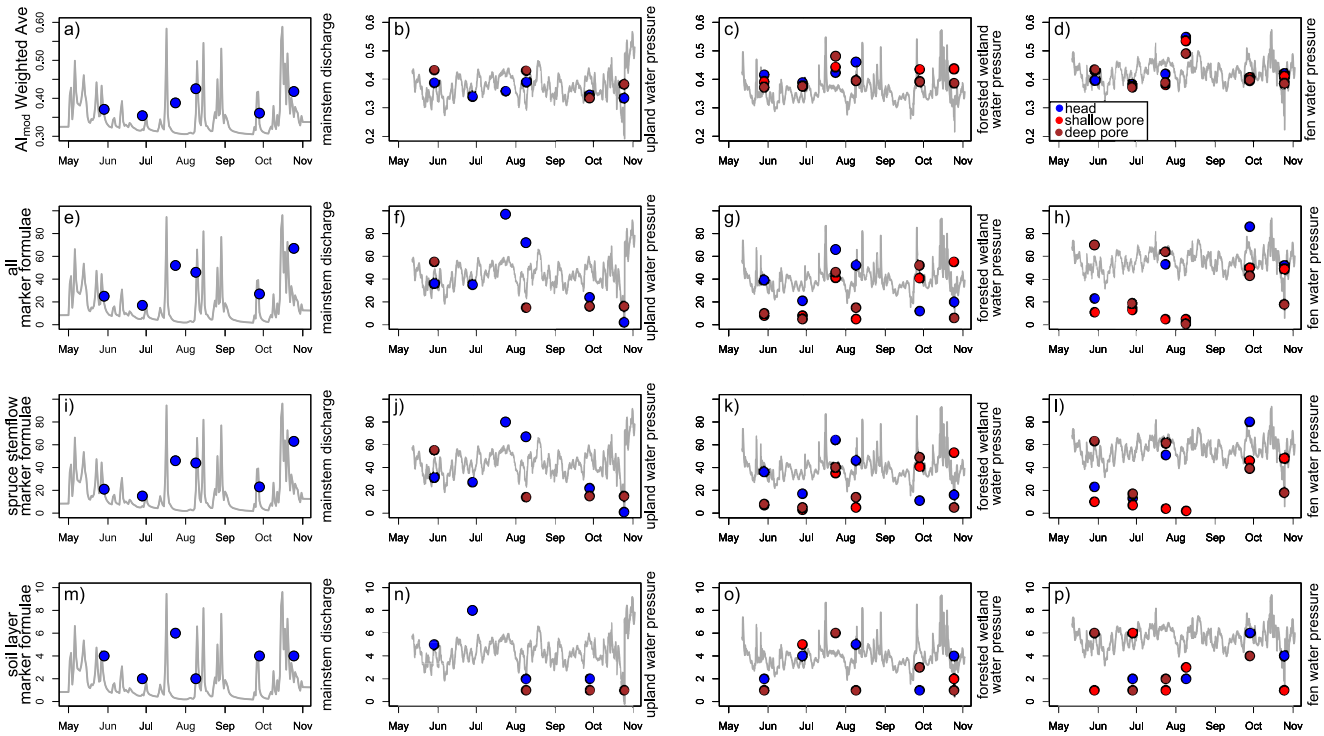

Figure 5. AI_{mod} (a–d), and total sum of all source-specific marker formulae (e–h), spruce stemflow marker formulae (i–l), and soil layer marker formulae (m–p) for sampling period. Mainstem (a,e,i,m), upland (b,f,j,n), forested wetland (c,g,k,o), and fen (d,h,l,p) data for stream samples (blue dots), shallow pore samples (red dots), and deep pore samples (brown dots). There were 281 total occurrences of marker formulae on the May sampling date, 133 in June, 424 in July, 215 in August, 353 in September, and 287 in October. For mainstem panels, Aangooxa Yé mainstem discharge is shown, while for sub-catchment panels sub-catchment water table pressure is shown. Water pressure and discharge are for reference and are not to scale.

precipitation, mainstem discharge, location of sample, and the reduced model with no independent variable, and their similar likelihood demonstrates there is more nuance to the number of source-specific formulae present than location and easily measurable continuous variables. Of the six models, only one (# of source-specific formulae ~ daily precipitation*location) showed a significant change ($p < 0.01$) in source-specific formulae by a factor of 0.554 for each additional cm of precipitation (0.371–0.860, 95% CI). However, model uncertainty meant that the model demonstrating the significance of precipitation for decreasing the number of source-specific formulae is not necessarily a more accurate model of the system than the other model candidates, including the fully reduced model with no explanatory variables. Similarly, when the number of occurrences of spruce stemflow-specific formulae was used as a model input for the same 12 linear models, five models had $\Delta AIC_c < 2$ and all of those models with continuous variables had $p > 0.50$ (Table S5 in the Supporting Information S1). Again, this included the reduced model with no independent variable, showing that the other models with low ΔAIC_c values (featuring location of sample, mainstem discharge, daily precipitation, and mean air temperature) were not capturing enough of the nuance regarding tree molecular formulae production to adequately describe the system.

Table 2
Number of Seasonal Unique Formulae Appearing in >1 Sampling Site for Each Month

Month	2 sites	3 sites	4 sites	5 sites
May	30	-	-	-
June	33	5	-	-
July	335	37	3	-
August	459	195	37	6
September	68	6	-	-
October	44	5	-	-

In contrast, only two of the 12 tested linear models explaining variance in the sum of specific marker formulae sourced from soil layers had $\Delta AIC_c < 2$, and both had $p < 0.01$ for at least one of their explanatory variables (Table S6 in the Supporting Information S1). The best model (AIC_c weight = 0.47) included an increase of ~0.7 specific marker formulae per cubic meter per second of mainstem discharge (0.57–0.90, 95%CI; $p < 0.01$). The other top model (AIC_c weight = 0.21) included an increase of ~0.7 specific marker formulae per cm precipitation (0.55–0.91; $p < 0.01$) and an increase of ~1.1 specific marker formulae per degree Celsius (1.00–1.15; $p = 0.05$). There was substantial support for one of 12 tested linear models explaining variance in AI_{mod} weighted average with $\Delta AIC_c > 17$ for all other tested models (Table

S7 in the Supporting Information S1). The best model included a small increase of ~0.03 units of AI_{mod} per cm of precipitation (0.00–0.05, 95%CI; $p = 0.07$) and an interaction term for site.

4. Discussion

4.1. Source-Specific Formulae Escape Degradation to Persist Downstream

All formulae previously identified as source-specific markers in Aangoo̲a Yé watershed were observed in this data set (Figure 5). The discovery of these marker formulae in the pore waters, tributary streams, and mainstem across the sampling period demonstrates that DOM in this watershed has not been entirely homogenized by abiotic removal processes or microbial degradation as has been hypothesized to occur in temperate watersheds (Harfmann et al., 2019). Instead, our findings agree with other studies suggesting that DOM produced in forest biomass or the soil profile can be shunted downstream to the mainstem relatively unaltered (Raymond et al., 2016). In our previous research, ~90% of source-specific marker formulae disappeared during a 14-day bioincubation, demonstrating high bioavailability under nutrient replete conditions (Behnke et al., 2022). Those 14-day incubations likely exceeded the residence time of water and DOM in sub-catchment in Aangoo̲a Yé, which are thought to be on the order of hours to a couple days (though exact residence times for the system are not known; Fellman, Hood, Edwards, & D'Amore, 2009; Fellman et al., 2020). The appearance of all the bioavailable source-specific formulae in this data set in soil pore waters and tributaries, and the mainstem suggests that: (a) residence times in the watershed are enough shorter than the 14-day bioincubations that microbes did not have enough time to process DOM along the terrestrial-stream continuum; (b) nutrient availability in situ was too low to allow microbial degradation; and/or 3) stationary bottle conditions in the incubation do not accurately mimic dynamic watershed processing. It is likely that the 14-day bottle bioincubation was a conservative indicator of stable formulae, and that marker formulae in situ escape degradation more easily.

Stemflow and throughfall (water running down trunks and dripping through branches; Van Stan & Stubbins, 2018) can have concentrations of DOC substantially exceeding those of most stream systems, especially in temperate and boreal regions (Fellman, Hood, D'Amore, et al., 2009; Hanley et al., 2013; Laudon et al., 2011; Mulholland, 1997; Pierre et al., 2020; Van Stan & Stubbins, 2018). These studies pose the question of whether tree DOM escapes terrestrial ecosystem degradation processes to contribute to stream DOM pools and potential export from catchments, either via through-soil flow, overland flow, or direct dripping of tree DOM into streams. The vast majority (>90%) of marker formulae occurrences in this sample set were sourced from spruce stemflow (Behnke et al., 2022) demonstrating that tree DOM not only occurs in tree stemflow and throughfall but that it can appear in downstream locations in the watershed. The discovery here of species- and source-specific tree DOM formulae in multiple locations along the catchment flowpath, including near the mouth of the mainstem, strongly suggests preservation of some tree DOM through the entire watershed and export to the receiving coastal marine waters in the NPCTR (Figures 5e–5h), especially since more tree DOM could be added from conifers growing along downstream stream reaches close to the mouth. It is possible that the source-specific marker formulae for tree DOM identified was in fact sourced along the catchment flowpath from some un-characterized endmember that shares these unique formulae with spruce stemflow. However, since the marker formulae were identified as formulae present in all samples taken from their source material and no samples of any other source material (e.g., tree or soil source leachates; Behnke et al., 2022), it is likely that these consistent and specific markers signal the presence of their specific tree DOM source. This finding highlights the importance of connectivity of terrestrial source pools and mainstem rivers and extends the terrestrial-marine continuum to include the forest canopy. If these same formulae were observed in the estuary or coastal ocean adjacent to the watershed, species-specific tree DOM could contribute to coastal ecosystem carbon cycling.

4.2. From Canopy to Coast: Seasonality and Antecedent Conditions Matter for Modeling Terrestrial Inputs

Our examination of the relationship between hydrology and four molecular indicators of fresh terrestrial DOM input (source-specific marker formulae, spruce stemflow-specific marker formulae, soil layer marker formulae (Behnke et al., 2022), and AI_{mod} weighted average; Figure 5) together demonstrate the complexity of characterizing a system with pronounced seasonal changes using simplistic hydrologic variables. The best model of AI_{mod} (AI_{mod} ~ daily precipitation * site) showed an increase of ~0.03 (0.00–0.05, 95%CI; $p = 0.07$) units of AI_{mod} per

cm of precipitation with an interaction term for site (Table S7 in the Supporting Information S1), suggesting that though the slope of the increase was different in different sub-catchments, precipitation unsurprisingly appears to modestly enhance the connectivity of headwater streams to terrestrial (e.g., high aromaticity) DOM source pools (DiDonato et al., 2016; Holt et al., 2021). Similarly, the two models that described soil layer marker formulae (sum ~ mainstem discharge; sum ~ daily precipitation * mean air temperature) show that increasing precipitation in the watershed (correlated to mainstem discharge) flushes DOM from soil layers into the stream system (Table S6 in the Supporting Information S1). Soil DOC can increase in concentration with rising temperature (e.g., Freeman et al., 2001; Wen et al., 2020), as seen here in the model relationship between increasing mean air temperature and soil layer marker formulae occurrences. The linkage between soil-derived DOM and watershed flow thus appears to involve both the movement of water and soil carbon availability.

In contrast to the model of soil layer marker formulae, there was model uncertainty for the full suite of source-specific marker formulae and for the sprue stemflow-specific marker formulae, and a lack of relationships for both with predictor variables for the majority of considered models (Tables S4 and S5 in the Supporting Information S1). The limited significance of these relationships argues that precipitation alone does not control molecular terrestrial connectivity when the full array of terrestrial DOM sources (plants as well as soil) is considered, and demonstrates that antecedent conditions, and the status of DOM sources (e.g., saturation state, growth stage), must also be considered for this and in similar watersheds (McMillan et al., 2018).

It is well established that riverine constituent processing reacts non-linearly to increasing discharge (Wollheim et al., 2018). Antecedent conditions have been shown to influence watershed responses to events through dictating source availability (e.g., how much fresh organic material is available to leach) and determining the flow path taken by water (e.g., fast flow through shallow surface soil layers vs. slow flow through deeper soil layers; D'Amore et al., 2015; McMillan et al., 2018; Raymond & Saiers, 2010; Tunaley et al., 2016; Wagner et al., 2019). Temperature and antecedent watershed hydrology can influence stream DOC concentrations (Raymond & Saiers, 2010) as demonstrated in the soil layer specific marker formulae, suggesting they are best at predicting soil derived DOM inputs. However, the myriad of biological processes at work within the soil column, the understory, and the canopy throughout the sampling period combine with temperature and hydrology to create a set of complex antecedents that influence DOM movement along the terrestrial-marine continuum. These conditions cannot be captured through simple metrics of hydrology and temperature alone when plant-derived DOM is considered along with soil-derived DOM in a holistic view of terrestrial inputs. Stream discharge itself is not always the best predictor of DOM production and export and can depend on more than precipitation (McMillan et al., 2018; Wollheim et al., 2018). High precipitation/discharge conditions encounter different states of DOM sources depending on the season (Tunaley et al., 2016) as well as the drying/wetting history of catchment soils (Raymond & Saiers, 2010), and at times hydrologic thresholds must be overcome to allow lateral movement of DOC from soil pore waters into streams (D'Amore et al., 2010).

While hysteresis is often invoked as a framework to think about antecedent hydrologic conditions (e.g., Sanderman et al., 2009; Wagner et al., 2019), we need a complementary framework to consider how plant growth stage impacts what biochemicals enter the DOM pool through leaching, and how fresh litter quantity and quality impact DOM chemistry. For example, low temperatures can increase conifer lipid content of needle cells (Nokhsorov et al., 2019; Pukacki & Kaminska-Rozek, 2013), and season can impact tree DOM aromaticity, suggesting export of different compounds at different moments (Levia et al., 2012). The biochemicals being leached from trees at any given moment will depend on plant production/senescence, and the transit time of tree DOM to streams depends on flow path and retention time of tree DOM in soils. These studies highlight the combined influence that multiple factors (e.g., temperature, plant activity, evapotranspiration, snowmelt, and other factors present at that moment) have in hydrology-DOM composition relationships. Higher frequency sampling than was logistically feasible in our sampling campaign and attention to more complex environmental variables would be needed to model the processes producing molecular terrestrial tracers at the small watershed scale.

4.3. Forested Wetland Pore Water Contains Unique Nitrogen Chemistry

Forested wetland pore waters have been suggested as active points of biogeochemical processing in the NPCTR (Bisbing & D'Amore, 2018; D'Amore et al., 2010). Previous work in wetland soils in the region has demonstrated that DON typically dominates soil water TDN pools (≥80%; Fellman, Hood, D'Amore, et al., 2009), as observed in other northern high-latitude or forested regions (Perakis & Hedin, 2002; Sponseller et al., 2014). Temperate

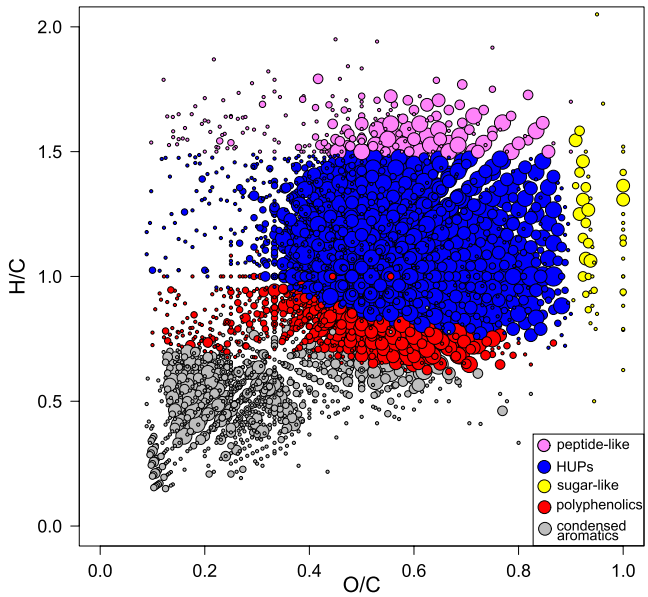

Figure 6. All 3,234 N-containing formulae that occur in forested wetland deep pore samples across the sampling period. Formulae are colored by compound class. Formula point sizes correspond to number of samples in which formula is present.

forested wetland soils typically produce larger amounts of DOC and DON than surrounding soils due to frequent water table and redox state fluctuations (which encourage SOM degradation) and greater inputs of fresh litter than adjacent fen sites due to the presence of trees (D'Amore et al., 2010; Fröberg et al., 2003). The forested wetland deep pore water had the highest mean DOC and TDN concentrations (33.3 ± 3.0 mgCL^{-1} and 2.2 ± 0.8 mgNL^{-1}) and lowest DOC:TDN (29.0 ± 10.3; Figure 2; Table 1). This ample nitrogen and DOM with a low DOC:TDN (indicative of bioavailable material; e.g., Wiegner & Seitzinger, 2004) can lead to microbial immobilization of nitrogen in the soil matrix, causing the highest DOC:TDN in the forested wetland headwater stream (Table 1; Figure 2; Bisbing & D'Amore, 2018).

Previous work in Japan and Sweden has demonstrated that microbial biomass increased throughout winter (Isobe et al., 2018) and freeze-thaw cycles increase soil nitrogen mineralization (Urakawa et al., 2014) contributing to a dissolved inorganic nitrogen (DIN) winter maximum that is maintained through low winter plant activity (Sponseller et al., 2014). We hypothesize that substantial microbial cell death and lysis occurred during the spring snowmelt, releasing DON (Isobe et al., 2018; Schimel & Clein, 1996). Thus, the release of DON and DIN from microbial cell lysis could explain the peak in TDN during May in our samples. Some of this microbially released DON may also be mineralized during snowmelt and subsequently taken up by plants in our study watershed, stimulating plant growth, as has been proposed in forested wetland soils in the NPCTR (D'Amore et al., 2009; Isobe et al., 2018).

Preferential uptake of DON such as amino acids by plant and/or microbial communities has been hypothesized to occur in the NPCTR as well as other high-latitude regions (Bennett & Prescott, 2004; Fellman, Hood, D'Amore, et al., 2009; Kielland, 1994; Neff et al., 2003), but the chemical composition of DON that might be available to uptake was unknown. Here, FT-ICR MS has confirmed the highest mean contribution of CHON-containing and peptide-like formulae of any site in forested wetland deep pore water sites (5.5 ± 0.5 and 0.3 ± 0.1%RA, respectively; Table 1), peaking in June (7.6 and 0.8%RA, respectively) following the TDN peak in May (5.9 mgNL^{-1}). The peak %RA of CHON-containing formulae occurring in June rather than in May could be due to the much higher DOC concentrations in the forested wetland deep pore site in May: loss of DOC to flushing during spring snowmelt may have removed more CHO-containing formulae than N-containing formulae, which can be preferentially retained in the soil matrix (Bisbing & D'Amore, 2018). Thus, though the %RA of CHON-containing formulae was highest in June, it is possible that the actual amount of them were higher in May and masked by high DOC concentration and substantial amounts of other formula types. A total of 3,234 N-containing formulae appear in forested wetland deep pore water samples (Figure 6), spanning all possible compound classes (by definition, aliphatics do not contain N). These N-containing formulae thus likely participate in multiple biotic and abiotic processes and demonstrate the wide range of compound categories that may be fulfilling the role of the easily mineralized or biologically available DON (Bennett & Prescott, 2004; Bisbing & D'Amore, 2018; Fellman, Hood, D'Amore, et al., 2009; Neff et al., 2003). A substantial fraction of this DON is present in peptide-like or sugar-like formulae, which are often highly bioavailable and whose high H/C ratios make them energy-rich (Hopkinson et al., 1998; Lawson et al., 2014; O'Donnell et al., 2016; Spencer et al., 2015; Textor et al., 2019). This biolabile DON may therefore be preferentially taken up by biota or preferentially mineralized, releasing DIN that could then be available for biotic uptake and nitrogen cycling.

4.4. Seasonal Patterns in the Degradation State of Terrestrial NPCTR DOM

Our findings that seasonal patterns in soil pore water and stream DOM concentration and composition are dictated by how much previous degradation terrestrial DOM has endured in this small NPCTR watershed is consistent with other temperate watershed-scale studies (Isobe et al., 2018; Sanderman et al., 2009; Wu et al., 2014). In our study watershed, colder temperatures and dormant plant activity likely allowed the buildup of TDN over winter in the soil matrix. Concentrations of TDN decreased throughout the course of the summer in the wetland soil pore

waters as biotic uptake increased and/or TDN was flushed to surface waters (Figures 3e–3h). Rewetting events during warm summer months appear to mobilize DOM with a freshly leached terrestrial signature and high molecular diversity to streams. As previously observed in wetlands, most sites showed increases in AI_{mod} and the %RA of polyphenolics and condensed aromatics spring to midsummer (Figures 5a–5d; Figure S2 in the Supporting Information S1), reflecting the aromatic, terrestrial nature of summer DOM source pools (Höll et al., 2009; Wiegner & Seitzinger, 2004).

Streamwater DOC concentrations increased up to >3.5 times low flow values during a noticeable rewetting event in August after a dry spell where DOM was able to accumulate in the soil matrix (Figures 3a–3d) (Kim et al., 2016; Miller et al., 2005; Tunaley et al., 2016; Worrall et al., 2002). July and August show substantially more month-specific formulae than do the earlier or later months (Table 2; Figure S3 in the Supporting Information S1), many of which are condensed aromatics and polyphenolics. These results further demonstrate the added diversity of fresh terrestrial summer DOM (DiDonato et al., 2016; Holt et al., 2021). All previously identified source-specific marker formulae (Behnke et al., 2022) appeared in the data set and spruce stemflow marker formulae dominated in the mainstem, demonstrating a freshly leached terrestrial signature and that tree DOM contributes to the mainstem near the catchment outlet to marine waters.

By fall, plant inputs and thus their leached material no longer contains freshly produced biomolecules and abundant precipitation decreases DOC concentrations through dilution. Month-specific unique formulae are minimal by October (Table 2; Figure S3 in the Supporting Information S1), and as previously noted, DOM becomes less diverse and more similar to spring DOM (Fellman, Hood, Edwards, & D'Amore, 2009). Unlike the Arctic paradigm where winter sets in and freezes relatively fresh material in place, which then provides a fresh terrestrial signature during spring freshet (Raymond et al., 2007; Striegl et al., 2007), winter in the NPCTR does not typically result in an extensive period (and depth) of soil freezing. Temperatures fluctuate around freezing at sea level, rain and snow alternate, and degraded and dormant organic matter continues to leach during rain events. Consistent molecular signatures reflective of more processed material persist through spring until the next summer provides more fresh terrestrial DOM. Future work should confirm that the degraded DOM signal also persists during winter.

In summary, we observed the basic seasonality of DOM composition within common NPCTR landscape units, with the potential for rapid transfer of DOM from specific terrestrial sources to the sea during high flow events. While soil-derived marker formulae showed a clearer relationship with hydrologic flushing and temperature, it appears that complex antecedent conditions dictate source availability and hydrologic connectivity, which in turn influence the presence of unique terrestrial DOM derived from plants along the stream network. Climate change in the NPCTR is likely to modify precipitation and temperature regimes and may decouple the timing of current seasons of hydrologic and biological activity and increase flushing of terrestrial source pools during increasing intense precipitation events in the region (Bidlack et al., 2021). Such changes will only further complicate modeling how source availability and hydrologic connectivity combine to dictate streamwater DOM composition, emphasizing the need for more high-resolution sampling campaigns to tease apart the controls on terrestrial DOM delivery to the ocean.

Data Availability Statement

All data used in this study are freely available on the Open Science Framework (https://osf.io/ry4ge/; DOI 10.17605/OSF.IO/RY4GE).

Acknowledgments

The authors thank Emily Whitney for her invaluable field, laboratory, and logistical assistance, Molly Tankersley for creating Figure 1, and Brian Davies of Eaglecrest Ski Area for the temperature and precipitation data. They also thank Clayton Williams and an anonymous reviewer for assistance improving the manuscript. This work was funded by the National Science Foundation through an NSF Graduate Research Fellowship to M. I. Behnke. A portion of this work was performed at the National High Magnetic Field Laboratory ICR User Facility, which is supported by the National Science Foundation Division of Chemistry and Division of Materials Research through DMR-1644779 and the State of Florida. The authors are grateful to the helpful researchers at the National High Magnetic Field Laboratory. This work took place on the lands of the Aak'w Kwáan Tlingit.

References

Behnke, M., Fellman, J., D'Amore, D., Gomez, S., & Spencer, R. (2022). From canopy to consumer: What makes and modifies terrestrial DOM in a temperate forest. *Biogeochemistry*, 1–21. https://doi.org/10.1007/s10533-022-00906-y

Behnke, M., Stubbins, A., Fellman, J. B., Hood, E., Dittmar, T., & Spencer, R. G. M. (2020). Dissolved organic matter sources in glacierized watersheds delineated through compositional and carbon isotopic modeling. *Limnology & Oceanography*, *66*, 438–451. https://doi.org/10.1002/lno.11615

Bennett, J. N., & Prescott, C. E. (2004). Organic and inorganic nitrogen nutrition of western red cedar, western hemlock and salal in mineral N-limited cedar–hemlock forests. *Oecologia*, *141*, 468–476. https://doi.org/10.1007/s00442-004-1622-3

Bercovici, S., Koch, B. P., Lechtenfeld, O. J., McCallister, S. L., Schmitt-Kopplin, P., & Hansell, D. (2018). Aging and molecular changes of dissolved organic matter between two deep oceanic end-members. *Global Biogeochemical Cycles*, *32*, 1449–1456. https://doi.org/10.1029/2017gb005854

Bhatia, M. P., Das, S. B., Longnecker, K., Charette, M. A., & Kujawinski, E. B. (2010). Molecular characterization of dissolved organic matter associated with the Greenland ice sheet. *Geochimica et Cosmochimica Acta*, *74*, 3768–3784. https://doi.org/10.1016/j.gca.2010.03.035

Bidlack, A. L., Bisbing, S. M., Buma, B. J., Diefenderfer, H. L., Fellman, J. B., Floyd, W. C., et al. (2021). Climate-mediated changes to linked terrestrial and marine ecosystems across the northeast Pacific coastal temperate rainforest margin. *BioScience*. https://doi.org/10.1093/biosci/biaa171

Bisbing, S. M., & D'Amore, D. V. (2018). Nitrogen dynamics vary across hydrologic gradients and by forest community composition in the perhumid coastal temperate rainforest of southeast Alaska. *Canadian Journal of Forest Research*, *48*, 180–191. https://doi.org/10.1139/cjfr-2017-0178

Buma, B., Krapek, J., & Edwards, R. T. (2016). Watershed-scale forest biomass distribution in a perhumid temperate rainforest as driven by topographic, soil, and disturbance variables. *Canadian Journal of Forest Research*, *46*, 844–854. https://doi.org/10.1139/cjfr-2016-0041

Burnham, K. P., & Anderson, D. R. (2002). A practical information-theoretic approach. In *Model selection and multimodel inference 2*.

Corilo, Y. (2015). PetroOrg. Florida State University.

D'Amore, D. V., Edwards, R. T., Herendeen, P. A., Hood, E., & Fellman, J. B. (2015). Dissolved organic carbon fluxes from hydropedologic units in Alaskan coastal temperate rainforest watersheds. *Soil Science Society of America Journal*, *79*, 378–388. https://doi.org/10.2136/sssaj2014.09.0380

D'Amore, D. V., Fellman, J. B., Edwards, R. T., & Hood, E. (2010). Controls on dissolved organic matter concentrations in soils and streams from a forested wetland and sloping bog in southeast Alaska. *Ecohydrology*, *3*, 249–261. https://doi.org/10.1002/eco.101

D'Amore, D. V., Hennon, P. E., Schaberg, P. G., & Hawley, G. J. (2009). Adaptation to exploit nitrate in surface soils predisposes yellow-cedar to climate-induced decline while enhancing the survival of western redcedar: A new hypothesis. *Forest Ecology and Management*, *258*, 2261–2268.

D'Andrilli, J., Junker, J. R., Smith, H. J., Scholl, E. A., & Foreman, C. M. (2019). DOM composition alters ecosystem function during microbial processing of isolated sources. *Biogeochemistry*, *142*, 281–298.

DiDonato, N., Chen, H., Waggoner, D., & Hatcher, P. G. (2016). Potential origin and formation for molecular components of humic acids in soils. *Geochimica et Cosmochimica Acta*, *178*, 210–222. https://doi.org/10.1016/j.gca.2016.01.013

Dittmar, T., Koch, B., Hertkorn, N., & Kattner, G. (2008). A simple and efficient method for the solid-phase extraction of dissolved organic matter (SPE-DOM) from seawater. *Limnology and Oceanography: Methods*, *6*, 230–235. https://doi.org/10.4319/lom.2008.6.230

Edwards, R. T., D'Amore, D. V., Biles, F. E., Fellman, J. B., Hood, E. W., Trubilowicz, J. W., & Floyd, W. C. (2021). Riverine dissolved organic carbon and freshwater export in the eastern Gulf of Alaska. *Journal of Geophysical Research: Biogeosciences*, *126*, e2020JG005725. https://doi.org/10.1029/2020JG005725

Fasching, C., Behounek, B., Singer, G. A., & Battin, T. J. (2014). Microbial degradation of terrigenous dissolved organic matter and potential consequences for carbon cycling in brown-water streams. *Scientific Reports*, *4*, 4981. https://doi.org/10.1038/srep04981

Fellman, J. B., D'Amore, D. V., Hood, E., & Boone, R. D. (2008). Fluorescence characteristics and biodegradability of dissolved organic matter in forest and wetland soils from coastal temperate watersheds in southeast Alaska. *Biogeochemistry*, *88*, 169–184. https://doi.org/10.1007/s10533-008-9203-x

Fellman, J. B., Hood, E., Behnke, M. I., Welker, J. M., & Spencer, R. G. (2020). Stormflows drive stream carbon concentration, speciation and dissolved organic matter composition in coastal temperate rainforest watersheds. *Journal of Geophysical Research: Biogeosciences*, e2020JG005804. https://doi.org/10.1029/2020JG005804

Fellman, J. B., Hood, E., D'Amore, D. V., Edwards, R. T., & White, D. (2009). Seasonal changes in the chemical quality and biodegradability of dissolved organic matter exported from soils to streams in coastal temperate rainforest watersheds. *Biogeochemistry*, *95*, 277–293. https://doi.org/10.1007/s10533-009-9336-6

Fellman, J. B., Hood, E., Edwards, R. T., & D'Amore, D. V. (2009). Changes in the concentration, biodegradability, and fluorescent properties of dissolved organic matter during stormflows in coastal temperate watersheds. *Journal of Geophysical Research*, *114*, G01021. https://doi.org/10.1029/2008JG000790

Ferguson, R. L., Buckley, E. N., & Palumbo, A. V. (1984). Response of marine bacterioplankton to differential filtration and confinement. *Applied and Environmental Microbiology*, *47*, 49–55. https://doi.org/10.1128/aem.47.1.49-55.1984

Flerus, R., Lechtenfeld, O., Koch, B. P., McCallister, S. L., Schmitt-Kopplin, P., Benner, R., et al. (2012). A molecular perspective on the ageing of marine dissolved organic matter. *Biogeosciences*, *9*, 1935–1955. https://doi.org/10.5194/bg-9-1935-2012

Freeman, C., Evans, C., Monteith, D., Reynolds, B., & Fenner, N. (2001). Export of organic carbon from peat soils. *Nature*, *412*, 785. https://doi.org/10.1038/35090628

Fröberg, M., Berggren, D., Bergkvist, B., Bryant, C., & Knicker, H. (2003). Contributions of Oi, Oe and Oa horizons to dissolved organic matter in forest floor leachates. *Geoderma*, *113*, 311–322.

Hanley, K. W., Wollheim, W. M., Salisbury, J., Huntington, T., & Aiken, G. (2013). Controls on dissolved organic carbon quantity and chemical character in temperate rivers of North America. *Global Biogeochemical Cycles*, *27*, 492–504. https://doi.org/10.1002/gbc.20044

Hansen, A. M., Kraus, T. E., Pellerin, B. A., Fleck, J. A., Downing, B. D., & Bergamaschi, B. A. (2016). Optical properties of dissolved organic matter (DOM): Effects of biological and photolytic degradation. *Limnology & Oceanography*, *61*, 1015–1032. https://doi.org/10.1002/lno.10270

Harfmann, J. L., Guillemette, F., Kaiser, K., Spencer, R. G., Chuang, C. Y., & Hernes, P. J. (2019). Convergence of terrestrial dissolved organic matter composition and the role of microbial buffering in aquatic ecosystems. *Journal of Geophysical Research: Biogeosciences*, *124*, 3125–3142. https://doi.org/10.1029/2018JG004997

Heath, L. S., Smith, J. E., Woodall, C. W., Azuma, D. L., & Waddell, K. L. (2011). Carbon stocks on forestland of the United States, with emphasis on USDA Forest Service ownership. *Ecosphere*, *2*, 1–21. https://doi.org/10.1890/ES10-00126.1

Hertkorn, N., Harir, M., Cawley, K. M., Schmitt-Kopplin, P., & Jaffé, R. (2016). Molecular characterization of dissolved organic matter from subtropical wetlands: A comparative study through the analysis of optical properties, NMR and FTICR/MS. *Biogeosciences*, *13*(8), 2257–2277. https://doi.org/10.5194/bg-13-2257-2016

Hertkorn, N., Ruecker, C., Meringer, M., Gugisch, R., Frommberger, M., Perdue, E. M., et al. (2007). High-precision frequency measurements: Indispensable tools at the core of the molecular-level analysis of complex systems. *Analytical and Bioanalytical Chemistry*, *389*, 1311–1327. https://doi.org/10.1007/s00216-007-1577-4

Höll, B. S., Fiedler, S., Jungkunst, H. F., Kalbitz, K., Freibauer, A., Drösler, M., & Stahr, K. (2009). Characteristics of dissolved organic matter following 20 years of peatland restoration. *Science of the Total Environment*, *408*, 78–83.

Holt, A. D., Fellman, J., Hood, E., Kellerman, A. M., Raymond, P., Stubbins, A., et al. (2021). The evolution of stream dissolved organic matter composition following glacier retreat in coastal watersheds of southeast Alaska. *Biogeochemistry*, 1–18. https://doi.org/10.1007/s10533-021-00815-6

Hopkinson, C. S., Buffam, I., Hobbie, J., Vallino, J., Perdue, M., Eversmeyer, B., et al. (1998). Terrestrial inputs of organic matter to coastal ecosystems: An intercomparison of chemical characteristics and bioavailability. *Biogeochemistry*, *43*, 211–234. https://doi.org/10.1023/A:1006016030299

Isobe, K., Oka, H., Watanabe, T., Tateno, R., Urakawa, R., Liang, C., et al. (2018). High soil microbial activity in the winter season enhances nitrogen cycling in a cool-temperate deciduous forest. *Soil Biology and Biochemistry*, *124*, 90–100. https://doi.org/10.1016/j.soilbio.2018.05.028

Johnston, S. E., Striegl, R. G., Bogard, M. J., Dornblaser, M. M., Butman, D. E., Kellerman, A. M., et al. (2020). Hydrologic connectivity determines dissolved organic matter biogeochemistry in northern high-latitude lakes. *Limnology & Oceanography*, *65*, 1764–1780. https://doi.org/10.1002/lno.11417

Kaiser, N. K., Quinn, J. P., Blakney, G. T., Hendrickson, C. L., & Marshall, A. G. (2011). A novel 9.4 Tesla FTICR mass spectrometer with improved sensitivity, mass resolution, and mass range. *Journal of the American Society for Mass Spectrometry*, *22*, 1343–1351. https://doi.org/10.1007/s13361-011-0141-9

Kellerman, A. M., Fo, G., Podgorski, D. C., Aiken, G. R., Butler, K. D., & Spencer, R. G. (2018). Unifying concepts linking dissolved organic matter composition to persistence in aquatic ecosystems. *Environmental Science and Technology*, *52*, 2538–2548. https://doi.org/10.1021/acs.est.7b05513

Kielland, K. (1994). Amino acid absorption by arctic plants: Implications for plant nutrition and nitrogen cycling. *Ecology*, *75*, 2373–2383. https://doi.org/10.2307/1940891

Kim, E.-A., Nguyen, H. V.-M., Oh, H. S., Hur, J., & Choi, J. H. (2016). Influence of soil conditions on dissolved organic matter leached from forest and wetland soils: A controlled growth chamber study. *Environmental Science and Pollution Research*, *23*, 5203–5213. https://doi.org/10.1007/s11356-015-5740-8

Koch, B., & Dittmar, T. (2006). From mass to structure: An aromaticity index for high-resolution mass data of natural organic matter. *Rapid Communications in Mass Spectrometry*, *20*, 926–932. https://doi.org/10.1002/rcm.2386

Koch, B., & Dittmar, T. (2016). From mass to structure: An aromaticity index for high-resolution mass data of natural organic matter. *Rapid Communications in Mass Spectrometry*, *20*, 926–932. https://doi.org/10.1002/rcm.7433

Koch, B., Dittmar, T., Witt, M., & Kattner, G. (2007). Fundamentals of molecular formula assignment to ultrahigh resolution mass data of natural organic matter. *Analytical Chemistry*, *79*, 1758–1763. https://doi.org/10.1021/ac061949s

Kurek, M. R., Garcia-Tigreros, F., Wickland, K. P., Frey, K. E., Dornblaser, M. M., Striegl, R. G., et al. (2023). Hydrologic and landscape controls on dissolved organic matter composition across western North American Arctic lakes. *Global Biogeochemical Cycles*, e2022GB007495. https://doi.org/10.1029/2022gb007495

Laudon, H., Berggren, M., Ågren, A., Buffam, I., Bishop, K., Grabs, T., et al. (2011). Patterns and dynamics of dissolved organic carbon (DOC) in boreal streams: The role of processes, connectivity, and scaling. *Ecosystems*, *14*, 880–893. https://doi.org/10.1007/s10021-011-9452-8

Lawson, E. C., Wadham, J. L., Tranter, M., Stibal, M., Lis, G. P., Butler, C. E. H., et al. (2014). Greenland ice sheet exports labile organic carbon to the Arctic oceans. *Biogeosciences*, *11*, 4015. https://doi.org/10.5194/bg-11-4015-2014

Lechtenfeld, O. J., Kattner, G., Flerus, R., McCallister, S. L., Schmitt-Kopplin, P., & Koch, B. P. (2014). Molecular transformation and degradation of refractory dissolved organic matter in the Atlantic and Southern Ocean. *Geochimica et Cosmochimica Acta*, *126*, 321–337. https://doi.org/10.1016/j.gca.2013.11.009

Levia, D. F., Van Stan, I., John, T., Inamdar, S. P., Jarvis, M. T., Mitchell, M. J., et al. (2012). Stemflow and dissolved organic carbon cycling: Temporal variability in concentration, flux, and UV-Vis spectral metrics in a temperate broadleaved deciduous forest in the eastern United States. *Canadian Journal of Forest Research*, *42*, 207–216. https://doi.org/10.1139/X11-173

Mazerolle, M. J. (2019). AICcmodavg: Model selection and multimodel inference based on (Q)AIC(c), R package version 2.2-2 edn

McMillan, S. K., Wilson, H. F., Tague, C. L., Hanes, D. M., Inamdar, S., Karwan, D. L., et al. (2018). Before the storm: Antecedent conditions as regulators of hydrologic and biogeochemical response to extreme climate events. *Biogeochemistry*, *141*, 487–501. https://doi.org/10.1007/s10533-018-0482-6

McNicol, G., Bulmer, C., D'Amore, D., Sanborn, P., Saunders, S., Giesbrecht, I., et al. (2019). Large, climate-sensitive soil carbon stocks mapped with pedology-informed machine learning in the North Pacific coastal temperate rainforest. *Environmental Research Letters*, *14*, 014004. https://doi.org/10.1088/1748-9326/aaed52

Miller, A. E., Schimel, J. P., Meixner, T., Sickman, J. O., & Melack, J. M. (2005). Episodic rewetting enhances carbon and nitrogen release from chaparral soils. *Soil Biology and Biochemistry*, *37*, 2195–2204. https://doi.org/10.1016/j.soilbio.2005.03.021

Mulholland, P. J. (1997). Dissolved organic matter concentration and flux in streams. *Journal of the North American Benthological Society*, *16*, 131–141. https://doi.org/10.2307/1468246

National Wetlands Working Group. (1988). Wetlands of Canada. In *Ecological land classification series, no. 24*. Sustainable Development Branch, Environment Canada, Ottawa, Ontario, and Polyscience Publications Inc, Montreal, Quebec 452.

Neff, J. C., Chapin, F. S., III, & Vitousek, P. M. (2003). Breaks in the cycle: Dissolved organic nitrogen in terrestrial ecosystems. *Frontiers in Ecology and the Environment*, *1*, 205–211. https://doi.org/10.1890/1540-9295(2003)001[0205:bitcdo]2.0.co;2

Nevalainen, L., Rantala, M. V., Kivilä, E. H., Lami, A., Wauthy, M., Rautio, M., & Luoto, T. P. (2020). Biogeochemical and photobiological responses of subarctic lakes to UV radiation. *Journal of Photochemistry and Photobiology B: Biology*, *209*, 111932. https://doi.org/10.1016/j.jphotobiol.2020.111932

Nokhsorov, V., Dudareva, L., & Petrov, K. (2019). Content and composition of lipids and their fatty acids in needles of Pinus sylvestris L. And Picea obovata Ledeb. upon cold hardening in the Cryolithozone of Yakutia. *Russian Journal of Plant Physiology*, *66*, 548–555. https://doi.org/10.1134/s1021443719040101

O'Donnell, J. A., Aiken, G. R., Butler, K. D., Guillemette, F., Podgorski, D. C., & Spencer, R. G. (2016). DOM composition and transformation in boreal forest soils: The effects of temperature and organic-horizon decomposition state. *Journal of Geophysical Research: Biogeosciences*, *121*, 2727–2744. https://doi.org/10.1002/2016JG003431

Opsahl, S., & Benner, R. (1997). Distribution and cycling of terrigenous dissolved organic matter in the ocean. *Nature*, *386*, 480–482. https://doi.org/10.1038/386480a0

Perakis, S. S., & Hedin, L. O. (2002). Nitrogen loss from unpolluted South American forests mainly via dissolved organic compounds. *Nature*, *415*, 416–419. https://doi.org/10.1038/415416a

Pierre, S. K. A., Oliver, A. A., Tank, S. E., Hunt, B. P. V., Giesbrecht, I., Kellogg, C. T. E., et al. (2020). Terrestrial exports of dissolved and particulate organic carbon affect nearshore ecosystems of the Pacific coastal temperate rainforest. *Limnology and Oceanography*, *65*, 2657–2675. https://doi.org/10.1002/lno.11538

Poulin, B. A., Ryan, J. N., Nagy, K. L., Stubbins, A., Dittmar, T., Orem, W., et al. (2017). Spatial dependence of reduced sulfur in everglades dissolved organic matter controlled by sulfate enrichment. *Environmental Science and Technology*, *51*, 3630–3639. https://doi.org/10.1021/acs.est.6b04142

Pukacki, P. M., & Kaminska-Rozek, E. (2013). Differential effects of spring reacclimation and deacclimation on cell membranes of Norway spruce seedlings. *Acta Societatis Botanicorum Poloniae*, *82*. https://doi.org/10.5586/asbp.2013.004

Raymond, P. A., McClelland, J., Holmes, R., Zhulidov, A. V., Mull, K., Peterson, B. J., et al. (2007). Flux and age of dissolved organic carbon exported to the arctic ocean: A carbon isotopic study of the five largest arctic rivers. *Global Biogeochemical Cycles*, *21*. https://doi.org/10.1029/2007GB002934

Raymond, P. A., & Saiers, J. E. (2010). Event controlled DOC export from forested watersheds. *Biogeochemistry*, *100*, 197–209. https://doi.org/10.1007/s10533-010-9416-7

Raymond, P. A., Saiers, J. E., & Sobczak, W. V. (2016). Hydrological and biogeochemical controls on watershed dissolved organic matter transport: Pulse-shunt concept. *Ecology*, *97*, 5–16. https://doi.org/10.1890/14-1684.1

R Core Team. (2019). *R: A language and environment for statistical computing*. R Foundation for Statistical Computing.

Rossel, P. E., Vähätalo, A. V., Witt, M., & Dittmar, T. (2013). Molecular composition of dissolved organic matter from a wetland plant (Juncus effusus) after photochemical and microbial decomposition (1.25 yr): Common features with deep sea dissolved organic matter. *Organic Geochemistry*, *60*, 62–71. https://doi.org/10.1016/j.orggeochem.2013.04.013

Sanderman, J., Lohse, K. A., Baldock, J. A., & Amundson, R. (2009). Linking soils and streams: Sources and chemistry of dissolved organic matter in a small coastal watershed. *Water Resources Research*, *45*. https://doi.org/10.1029/2008wr006977

Schimel, J. P., & Clein, J. S. (1996). Microbial response to freeze-thaw cycles in tundra and taiga soils. *Soil Biology and Biochemistry*, *28*, 1061–1066. https://doi.org/10.1016/0038-0717(96)00083-1

Seidel, M., Yager, P. L., Ward, N. D., Carpenter, E. J., Gomes, H. R., Krusche, A. V., et al. (2015). Molecular-level changes of dissolved organic matter along the Amazon river-to-ocean continuum. *Marine Chemistry*, *177*, 218–231. https://doi.org/10.1016/j.marchem.2015.06.019

Shirokova, L. S., Chupakov, A. V., Zabelina, S. A., Neverova, N. V., Payandi-Rolland, D., Causserand, C., et al. (2019). Humic surface waters of frozen peat bogs (permafrost zone) are highly resistant to bio-and photodegradation. *Biogeosciences*, *16*, 2511–2526. https://doi.org/10.5194/bg-16-2511-2019

Sleighter, R. L., & Hatcher, P. G. (2008). Molecular characterization of dissolved organic matter (DOM) along a river to ocean transect of the lower chesapeake bay by ultrahigh resolution electrospray ionization fourier transform ion cyclotron resonance mass spectrometry. *Marine Chemistry*, *110*, 140–152. https://doi.org/10.1016/j.marchem.2008.04.008

Spencer, R. G., Mann, P. J., Dittmar, T., Eglinton, T. I., McIntyre, C., Holmes, R. M., et al. (2015). Detecting the signature of permafrost thaw in Arctic rivers. *Geophysical Research Letters*, *42*, 2830–2835. https://doi.org/10.1002/2015GL063498

Sponseller, R. A., Temnerud, J., Bishop, K., & Laudon, H. (2014). Patterns and drivers of riverine nitrogen (N) across alpine, subarctic, and boreal Sweden. *Biogeochemistry*, *120*, 105–120. https://doi.org/10.1007/s10533-014-9984-z

Stenson, A. C., Marshall, A. G., & Cooper, W. T. (2003). Exact masses and chemical formulas of individual Suwannee river fulvic acids from ultrahigh resolution electrospray ionization fourier transform ion cyclotron resonance mass spectra. *Analytical Chemistry*, *75*, 1275–1284. https://doi.org/10.1021/ac026106p

Stets, E. G., & Striegl, R. G. (2012). Carbon export by rivers draining the conterminous United States. *Inland Waters*, *2*, 177–184. https://doi.org/10.5268/iw-2.4.510

Striegl, R. G., Dornblaser, M. M., Aiken, G. R., Wickland, K. P., & Raymond, P. A. (2007). Carbon export and cycling by the Yukon, Tanana, and Porcupine rivers, Alaska, 2001–2005. *Water Resources Research*, *43*. https://doi.org/10.1029/2006wr005201

Stubbins, A., & Dittmar, T. (2015). Illuminating the deep: Molecular signatures of photochemical alteration of dissolved organic matter from North Atlantic deep water. *Marine Chemistry*, *177*, 318–324. https://doi.org/10.1016/j.marchem.2015.06.020

Stubbins, A., Silva, L. M., Dittmar, T., & Van Stan, J. T. (2017). Molecular and optical properties of tree-derived dissolved organic matter in throughfall and stemflow from live oaks and eastern red cedar. *Frontiers of Earth Science*, *5*, 22. https://doi.org/10.3389/feart.2017.00022

Textor, S., Wickland, K., Podgorski, D., Johnston, S. E., & Spencer, R. G. M. (2019). Dissolved organic carbon turnover in permafrost-influenced watersheds of interior Alaska: Molecular insights and the priming effect. *Frontiers of Earth Science*, *7*, 275. https://doi.org/10.3389/feart.2019.00275

Tunaley, C., Tetzlaff, D., Lessels, J., & Soulsby, C. (2016). Linking high-frequency DOC dynamics to the age of connected water sources. *Water Resources Research*, *52*, 5232–5247. https://doi.org/10.1002/2015wr018419

Urakawa, R., Shibata, H., Kuroiwa, M., Inagaki, Y., Tateno, R., Hishi, T., et al. (2014). Effects of freeze–thaw cycles resulting from winter climate change on soil nitrogen cycling in ten temperate forest ecosystems throughout the Japanese archipelago. *Soil Biology and Biochemistry*, *74*, 82–94. https://doi.org/10.1016/j.soilbio.2014.02.022

Van Stan, J. T., & Stubbins, A. (2018). Tree-DOM: Dissolved organic matter in throughfall and stemflow. *Limnology and Oceanography Letters*. https://doi.org/10.1002/lol2.10059

Van Stan, J. T., Wagner, S., Guillemette, F., Whitetree, A., Lewis, J., Silva, L., & Stubbins, A. (2017). Temporal dynamics in the concentration, flux, and optical properties of tree-derived dissolved organic matter in an epiphyte-laden oak-cedar forest. *Journal of Geophysical Research: Biogeosciences*, *122*, 2982–2997. https://doi.org/10.1002/2017JG004111

Venables, W. N., & Ripley, B. D. (2002). *Modern applied statistics with S* (4th ed.). Springer.

Wagner, S., Fair, J. H., Matt, S., Hosen, J. D., Raymond, P., Saiers, J. H., et al. (2019). Molecular hysteresis: Hydrologically driven changes in riverine dissolved organic matter chemistry during a storm event. *Journal of Geophysical Research: Biogeosciences*, *124*, 759–774. https://doi.org/10.1029/2018JG004817

Walvoord, M. A., & Striegl, R. G. (2007). Increased groundwater to stream discharge from permafrost thawing in the Yukon river basin: Potential impacts on lateral export of carbon and nitrogen. *Geophysical Research Letters*, *34*. https://doi.org/10.1029/2007gl030216

Wen, H., Perdrial, J., Abbott, B. W., Bernal, S., Dupas, R., Godsey, S. E., et al. (2020). Temperature controls production but hydrology regulates export of dissolved organic carbon at the catchment scale. *Hydrology and Earth System Sciences*, *24*, 945–966. https://doi.org/10.5194/hess-24-945-2020

Wiegner, T. N., & Seitzinger, S. P. (2004). Seasonal bioavailability of dissolved organic carbon and nitrogen from pristine and polluted freshwater wetlands. *Limnology & Oceanography*, *49*, 1703–1712. https://doi.org/10.4319/lo.2004.49.5.1703

Wollheim, W. M., Bernal, S., Burns, D. A., Czuba, J. A., Driscoll, C. T., Hansen, A. T., et al. (2018). River network saturation concept: Factors influencing the balance of biogeochemical supply and demand of river networks. *Biogeochemistry*, *141*, 503–521. https://doi.org/10.1007/s10533-018-0488-0

Worrall, F., Burt, T., Jaeban, R., Warburton, J., & Shedden, R. (2002). Release of dissolved organic carbon from upland peat. *Hydrological Processes*, *16*, 3487–3504. https://doi.org/10.1002/hyp.1111

Wu, H., Peng, C., Moore, T., Hua, D., Li, C., Zhu, Q., et al. (2014). Modeling dissolved organic carbon in temperate forest soils: TRIPLEX-DOC model development and validation. *Geoscientific Model Development*, *7*, 867–881. https://doi.org/10.5194/gmd-7-867-2014

Yang, Y.-Y., Tfaily, M. M., Wilmoth, J. L., & Toor, G. S. (2022). Molecular characterization of dissolved organic nitrogen and phosphorus in agricultural runoff and surface waters. *Water Research*, *219*, 118533. https://doi.org/10.1016/j.watres.2022.118533